Accurate calibration framework for the discrete element parameters of red kidney bean using flower pollination algorithm

Xuezhen Wang*, Kaiyuan Gu, Jiangtao Ji

(*College of Agricultural Equipment Engineering, Henan University of Science and Technology, Luoyang 471000, Henan, China*)

Abstract: Accurate calibration of discrete element method (DEM) parameters is essential for simulating the mechanical behavior of crop seeds and their interactions with agricultural equipment. However, most DEM parameters for red kidney beans (RKBs) remain unreported, and accuracy of conventional calibration methods still require further improvement. This study developed an accurate calibration approach for determining DEM parameters of RKBs. Physical properties of RKBs, including dimensional characteristics, densities, and frictional parameters, were first measured through laboratory experiments. Significant DEM parameters affecting the repose angle (RPA) were identified using the Plackett-Burman design, and their relationships with RPA were established using the Central Composite design. The optimal combination of parameters was then determined through grey wolf optimizer (GWO) and flower pollination algorithm (FPA). The results showed that moment of 12 s for RPA measurement and lifting velocity of 0.014 m/s were determined on aspects of higher accuracy in measuring repose angles and relatively less computation time and memory of usage in raising cylinder method simulations. An optimal combination of significant DEM parameters of RKBs is coefficient of static friction of 0.1338 and coefficient of rolling friction of 0.0308 optimized using flower pollination algorithm (FPA). The relative error between simulated and measured RPAs is 0.90% and the difference between simulated and measured RPAs did not reach a significant level (p>0.05). These results imply that the proposed calibration method effectively improves model accuracy, providing a reliable reference for DEM parameter calibration of crop seeds and supporting the design of RKB-related mechanized systems.

Keywords: raising cylinder method (RCM), discrete element method (DEM), parameter calibration, red kidney bean (RKB), flower pollination algorithm (FPA)

DOI: 10.25165/j.ijabe.20261904.10510

Citation: Wang X Z, Gu K Y, Ji J T. Accurate calibration framework for the discrete element parameters of red kidney bean using flower pollination algorithm. Int J Agric & Biol Eng, 2026; 19(4): 43–50.

1 Introduction

Red kidney bean (RKB), biologically known as the phaseolus vulgaris, belongs to the leguminous family and butterfly flower subfamily. The RKB is rich in a variety of essential amino acids, dietary fiber, essential minerals, and trace elements that the human body needs[1,2]. It can effectively improve people's diet structure and prevent a variety of diseases. At the same time, RKB has high medicinal value and is welcomed by domestic and foreign markets, as indicated by its share in 20%-25% of the entire edible bean export volume in international trade. According to the survey report of the International Food and Agriculture Organization (FAO), RKB is the second bean variety in the international planting area, and the global total planting area is second only to soybean[1]. However, the current mechanization level of RKB is still very low as rare agricultural machineries are available for the RKB[2]. As a result, the sowing, harvesting, and post-processing operations of the RKB require a lot of labor and energy input, which is not conducive to the sustainable development of modern agriculture. Understanding the interactions between RKB seeds and equipment is essential for designing high-performance agricultural machineries for RKBs, which was still absent in previous studies[3-5].

Three methods are commonly employed for investigating seed-equipment interactions, namely empirical and experimental methods and numerical simulation method. Although actual lab measurements of seed dynamic behaviors and empirical observations may give foundational insights, they are generally expensive and time-consuming. Recently, simulation methods like finite element method (FEM) have been proposed. However, the general limitation of the FEM is that it commonly accounts for total deformation of an object instead of predicting seed behaviors at particle levels, resulting in problems of accuracy and convergence[6].

The discrete element method (DEM) emerged in 1971 and subsequently was applied to the research of soil mechanics by Cundall and Strack[6]. PFC (i.e., Particle Flow Code) is the first commercial general-purpose discrete element software, firstly introduced in 1994 by the ITASCA engineering consulting company co-founded by Cundall. PFC is a command flow-based operation interface. Operation of this software needs to firstly master its built-in FISH language and command instructions to achieve human-computer interaction[6]. Another commercial discrete element software is EDEM (Experts in Discrete Element Modeling) (DEM Solutions Ltd. Edinburgh, Scotland, UK)[5,7,8]. Compared with PFC, EDEM realizes all graphical operations in the whole simulation process (i.e., modeling, solving, and post-processing), making EDEM highly practical and easy to learn[6]. Parameters required for running DEM simulations mainly include contact and intrinsic parameters[5]. The efficiency and accuracy for calibrating these parameters can significantly affect the understanding of agricultural parts-crop seeds interactions. Historically, the trial and error method (TEM) has been the primary approach for calibrating

Received date: 2026-02-26 **Accepted date:** 2026-07-20

Biographies: Kaiyuan Gu, Senior undergraduate, research interest: agricultural engineering, Email: 2675980291@qq.com; **Jiangtao Ji**, PhD, Professor, research interest: agricultural engineering, Email: jjt0907@163.com.

***Corresponding author: Xuezhen Wang**, PhD, Associate Professor, research interest: agricultural engineering. No. 48, Xiyuan Road, Jianxi District, Luoyang 471000, Henan, China. Tel: +86-13689243126, Email: xzwang@nwsuaf.edu.cn.

the DEM parameters. A typical example of TEM application is a study from Chen et al.[8], who determined particle stiffness of three soil types by varying it until the relative error between measured and simulated forces reached a minimum value. Other common response indices used for calibrating DEM parameters of various agricultural particles include soil rupture distance ratio[9], tillage forces[10], and repose angle[11]. The major disadvantage of TEM is that it is time-consuming and inefficient, especially when values of many parameters are uncertain or cannot be determined through physical tests. A novel method of combining a list of DEM simulations was subsequently introduced and preferred[5]. Zhu et al.[12] calibrated coefficients of inner static friction and inner rolling friction and surface energy of lunar soil by combining actual measurements and a series of DEM simulations. Wang et al.[5] proposed a method for determining DEM parameters of a loose cohesive soil with various moisture contents. Li et al.[13] employed funneling repose angle method to calibrate DEM parameters of wheat flour, and the accuracy was validated using relative error between actual and simulated repose angles. Hu et al.[14] developed the discrete element bonded-particle model of cotton seeds based on DEM and CFD coupling simulation and calibrated it by physical tests and Box-Behnken simulations. Results from the above review revealed that no literature associated with DEM parameters of RKB model was found. Moreover, effects of structural and working parameters (e.g., lifting velocity and measuring moment for repose angles) were rarely investigated in parameter calibration of different agricultural particles. While the method of combining tests offers a standardized process for parameter calibration of agricultural granular materials, the calibrated DEM parameters may exhibit relatively high relative errors (exceeding 4.9%-8.2%)[15,16].

Swarm intelligence optimization algorithms (SIOA) offer an efficient alternative for parameter calibration. These stochastic algorithms mimic the collective behaviors of animal groups, such as migration and foraging, to identify optimal solutions[17,18]. SIOA exhibit strong global search capability, adaptability, and parallelism, making them well suited for calibrating DEM parameters of agricultural granular bulk materials (e.g., red kidney bean) accurately. For example, the grey wolf optimizer (GWO) mimics social hierarchy and cooperative hunting behaviors (encircling, chasing, and attacking prey) of grey wolf packs in nature[18]. Flower pollination algorithm (FPA) is inspired by the flower pollination process, modeling both the long-distance global pollination (carried by pollinators) and local pollination (self-pollination or pollination within a limited vicinity) of flowering plants[19].

Thus, the aims of this study were to (1) investigate the impact of lifting velocity and measuring moment on repose angles of RKB, (2) obtain reasonable ranges of DEM parameters which significantly affected repose angles through Plackett-Burman and Steepest Climb simulations, (3) optimize significant DEM parameters of RKB using GWO and FPA, and (4) propose an accurate calibration framework applicable to RKBs and other agricultural particles.

2 Materials and methods

2.1 Lab measurement of red kidney beans

A total of 500 red kidney beans (RKBs) were randomly selected for measuring their 3D dimensions, including RKB length (L), RKB width (W), and RKB thickness (T) (Figure 1a). The particle density of RKB was measured according to the mass (M_{rkb}) per unit volume of RKBs using the measuring cylinder method (Figure 1b): initially, some RKB seeds were weighed to determine their mass; then these RKB seeds were poured into a measuring cylinder with some water; the total volume of these RKB particles was therefore obtained in accordance with the change in water surface before and after pouring RKB seeds.

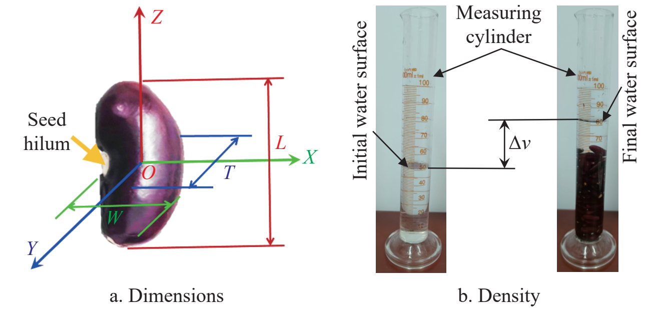

Note: L=RKB length; W=RKB width; T=RKB thickness; Δv stands for the difference between initial and final water surface.

Figure 1 Measurement of three dimensions and particle density of red kidney bean (RKB)

The thousand kernel weight (TKW) of RKB was determined as the total mass of 1000 RKBs[20]. Measurements of both bulk density and TKW were repeated three times. Feasible ranges of elastic modulus and Poisson's ratio of the RKB were estimated by a combination of the material database of EDEM and previous literature[21-23].

Contact parameters of the RKB consist of coefficient of restitution (R_{co}), coefficient of static friction (S_{fc}), and coefficient of rolling friction (R_{fc})[5]. The R_{co} mainly reflects the macro variation of velocities before and after collisions. It is generally defined as the ratio of the velocity after collision and that before collision. The specific measurement method of R_{co} is shown in Figure 2. The initial height H of RKB seed before dropping is 0.5 m. The RKB seed was released with an initial velocity of zero, and then it fell vertically and eventually rebounded upwards after colliding with an RKB sheet or acrylic glass sheet. The largest height of RKB after the first collision is h, which was recorded by a camera. Therefore, R_{co} was determined, as shown in Equation (1):

$$R_{co}=\frac{v_a}{v_b}=\sqrt{\frac{2gh}{2gH}}=\sqrt{\frac{h}{H}} \tag{1}$$

where, g represents gravitational acceleration (9.8 m/s^2); v_a and v_b stand for RKB velocities after and before collisions, respectively.

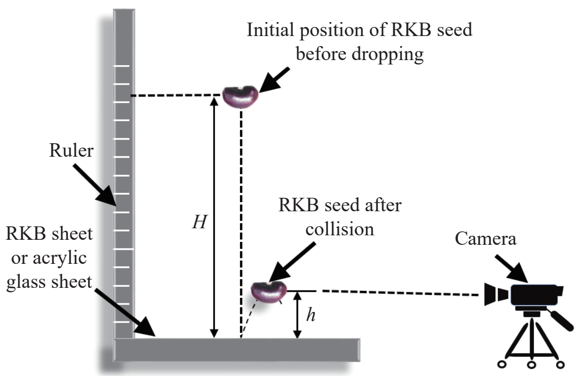

Figure 2 Diagram for measuring the restitution coefficient of red kidney bean (RKB)

Static friction coefficient (S_{fc}) between RKB and acrylic glass sheet (AGS) was measured by inclined sheet test, as shown in Figure 3a. Initially, a sheet of seeds (SOS) made of nine RKB seeds was placed on an AGS. The AGS then rotated around the rotational shaft. The angle (α) between the horizontal line and travel direction of SOS was collected when SOS began to move. The S_{fc} was calculated according to the tangent value of the α. The S_{fc} between RKB particles was measured using similar procedures.

Coefficient of rolling friction (R_{fc}) of RKB-AGS was measured in accordance with the conservation law of mechanical energy. The measurement method is shown in Figure 3b. Initially an RKB seed was placed on the inclined AGS, and the distance between the original position of RKB seed and the rotational shaft is d_i. The RKB seed then rolled forward and down under the combined action of gravitational and rolling friction forces. It eventually stopped after a distance (d_h) rolling on the horizontal AGS due to the rolling friction force between RKB and AGS. The specific equation for calculating R_{fc} between RKB and AGS is as follows:

$$R_{fc}=d_i\sin\theta/(d_i\cos\theta+d_h) \tag{2}$$

where, θ is the angle between travel direction of RKB seed and horizontal line, (°). The R_{fc} between RKB particles was measured using similar procedures.

The raising cylinder method (RCM) was performed to obtain the repose angle (RPA) of RKBs (Figure 4), which was commonly used in previous studies[24,25]. Initially, a cylinder filled with RKBs was raised vertically; then the RKBs flowed out of the cylinder (i.e., moments 1 and 2 in Figure 4), gradually producing a cone of RKB seeds. The cone image was taken when no noticeable movement of RKB was found. Once the cone stabilized, an image was captured facing the cone directly. The cone image was then imported into AutoCAD 2018 software. Using the software's spline function, the right and left boundaries of the conical pile was traced. The DATAEXTRACTION command was employed to export the coordinate points of the two spline curves to a ".csv" file. This file was subsequently opened in Excel software. Finally, linear regression was performed on the extracted coordinate data. The absolute value of the slope obtained from this linear fit corresponds to the tangent of the RPA for the RKB cone. Each test was repeated three times, and the average of six RPA measurements was used for DEM parameter calibration.

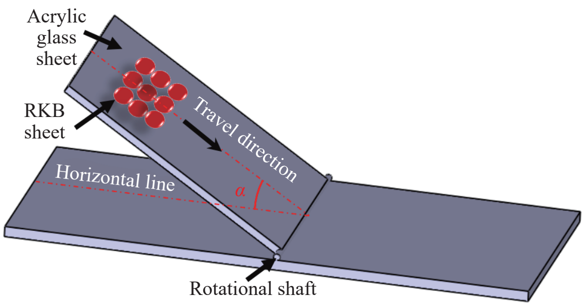

a. Static friction coefficient b. Rolling friction coefficient

Note: AGS represents acrylic glass sheet; d_i, d_h, and θ represent distance between original position of RKB seed and rotational shaft, distance between final position of RKB seed and rotational shaft, and angle between travel direction of RKB seed and horizontal line.

Figure 3 Diagram for measuring the coefficients of static friction and rolling friction of red kidney bean (RKB)

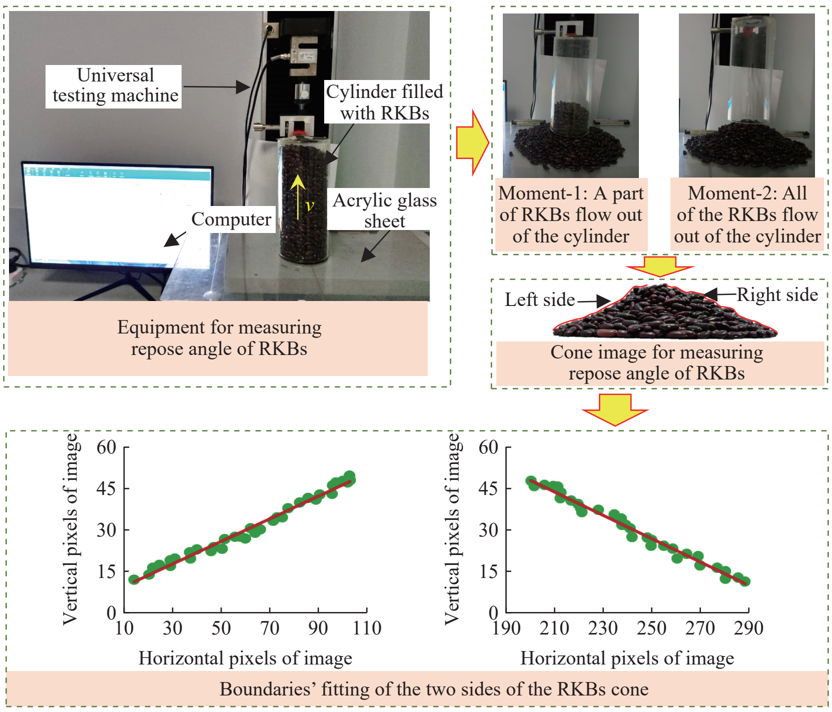

Figure 4 Repose angle measurement of red kidney beans (RKBs) in the lab

2.2 DEM modeling of red kidney beans

2.2.1 Determination of the repose angle of RKB

The DEM model of RKB seed (Figure 5a) was developed using seven spheres, and their coordinates are listed in Table 1. The contact between RKB seeds and between RKB seed and acrylic glass sheet is Hertz-Mindlin (no slip).

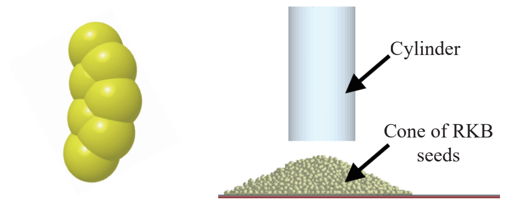

a. DEM model b. Repose angle simulation

Figure 5 DEM model of red kidney bean (RKB) and repose angle simulation using the raising cylinder method (RCM)

Table 1 Spherical particle coordinates for constructing the red kidney bean seed model

Particle No.	X/mm	Y/mm	Z/mm	R/mm
1	–5.126 08	–0.737 998	0.001 023	2.825
2	–1.710 11	–0.437 636	0.000 504 428	2.825
3	1.706 89	–0.437 273	9.96663e-05	2.825
4	5.123 92	–0.736 911	–0.000 191 162	2.825
5	–3.001 24	0.791 227	0.000 190 607	2.825
6	–0.001 305 33	1.399 55	–0.000 395 664	2.825
7	2.998 76	0.791 864	–0.000 520 125	2.825

The raising cylinder method (RCM) simulations were also performed to obtain the cones of RKB seeds in DEM (Figure 5b), and simulated repose angles (RPAs) were obtained using the same method shown in Figure 4. Each simulation was repeated three times.

2.2.2 Effects of lifting velocity and measurement moment

Variation of velocity can result in change in simulation time for computation, memory of usage, and accuracy of the RPA due to different kinetic and potential energies. At the same time, measurement moment of the RPA also affects the accuracy for running the simulations and the measurement of the RPA. For example, too early measurement can lead to inaccurate RPAs as subsequent movement of RKB particles may vary the RPA; too late measurement of the RPA can raise the total running time of simulations and corresponding memory of usage. To accurately obtain RPAs in an efficient manner, effects of lifting velocity and measurement moment of the RPA were investigated. The optimal lifting velocity and measurement moment were applied in RCM simulations and measurements.

2.3 Calibration of DEM parameters of RKB

The lab repose angle (RPA) tests of red kidney beans were also performed using the RCM. Measurement method of RPAs obtained in the lab is the same as that in DEM simulations. The measured repose angles were employed to calibrate model parameters of RKB. Initially, significant DEM parameters of RKB were screened using Plackett-Burman (PLB) test according to their effects on the RPA. The Steepest Ascent (STA) test was used to acquire their more reasonable ranges. The relationship between these significant parameters and RPA was established using the Central Composite (CEC) test.

The Grey Wolf Optimizer (GWO) and Flower Pollination Algorithm (FPA) were then employed to optimize the significant DEM parameters. The optimization was performed by minimizing the relative error (RE) between the predicted and measured RPAs (Equation (3)). The accuracy of the optimized parameters was further validated using both the relative error and the *p*-value obtained from a *t*-test.

$$RE = \frac{|RPA_p - RPA_m|}{RPA_m} \times 100\% \tag{3}$$

where, RPA_p is predicted repose angle; RPA_m is measured repose angle.

Figure 6 summarizes the overall methodology, including experimental measurements, model development, and parameter calibration.

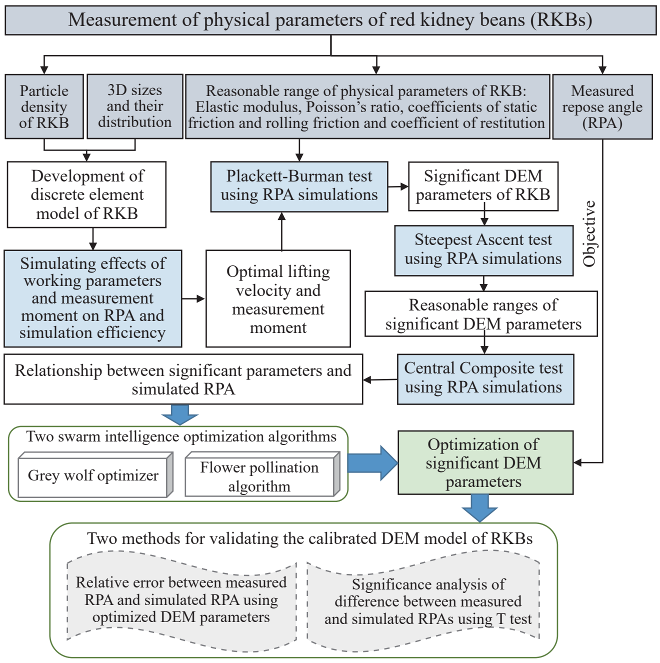

Figure 6 Flowchart illustrating the overall data processing procedure of red kidney beans

3 Results and discussion

3.1 Results from lab measurement

Three normal distributions were found for the number and frequency of RKBs on aspects of width (*W*), length (*L*), and thickness (*T*), as shown in Figure 7. Average values of *W*, *L*, and *T* from repeated measurements were 15.90 mm, 7.79 mm, and 5.65 mm, respectively.

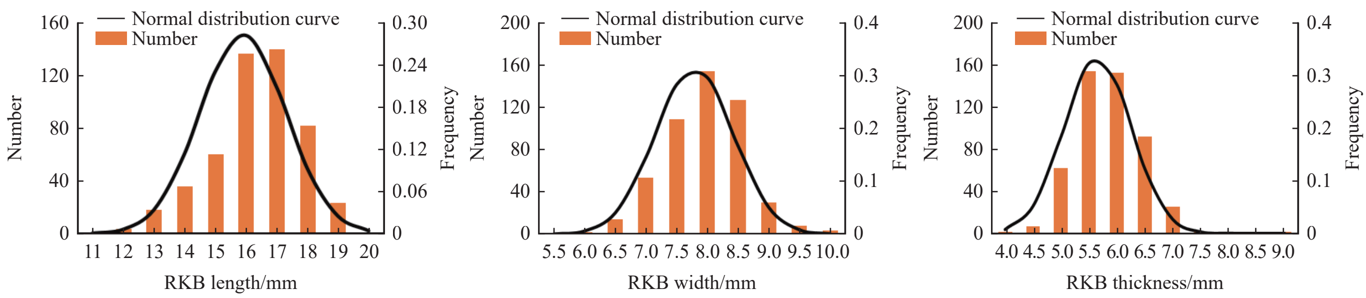

a. RKB length b. RKB width c. RKB thickness

Figure 7 Dimension distributions of red kidney bean (RKB)

The ranges of Poisson's ratio and elastic modulus of the RKB were 0.2-0.4 and 13-17 MPa, respectively. Ranges of coefficient of restitution, coefficient of static friction, and coefficient of rolling friction between RKB and acrylic glass sheet were 0.19-0.55, 0.22-0.559, and 0.02-0.16, respectively. The major DEM parameters are listed in Table 2.

Table 2 Major DEM parameters of the red kidney bean (RKB)

Parameter	Value
Poisson's ratio of RKB	0.2-0.4
Elastic modulus of RKB/MPa	13-17
Density of RKB/kg·m^{-3}	1271
Poisson's ratio of acrylic glass	0.33
Shear modulus of acrylic glass/MPa	82
Density of acrylic glass/kg·m^{-3}	1219
Coefficient of restitution between RKBs	0.13-0.37
Coefficient of static friction between RKBs	0.1-0.7
Coefficient of rolling friction between RKBs	0.02-0.22
Coefficient of restitution between RKB and acrylic glass	0.19-0.55
Coefficient of static friction between RKB and acrylic glass	0.22-0.59
Coefficient of rolling friction between RKB and acrylic glass	0.02-0.16

3.2 Effects of lifting velocity and measurement moment

3.2.1 Effect of lifting velocity

Effect of lifting velocity of cylinder in the raising cylinder method (RCM) on the formation of RKB cone, simulation time, and memory of usage was investigated. With the increase in lifting velocity from 0.004 to 0.054 m/s, an overall decreasing trend of RPA was found and the difference did not reach a significant level. Moreover, simulation time and memory of usage were reduced rapidly when lifting velocity was increased from 0.004 to 0.014 m/s (Figure 8). A lifting velocity of 0.014 m/s was determined for the DEM simulation of RCM by considering RPA accuracy and requirements of simulation time and memory of usage.

3.2.2 Effect of measurement moment

In DEM simulations, the RKB was produced initially at the top of the cylinder and then fell gradually under the action of gravity (Figures 9a and 9b); in the process, kinetic energy initially increased and then decreased (Figure 10a). The kinetic energy disappeared when the cylinder was full of RKB seeds at the moment of 1.9 s (Figures 9c and 10a), which indicated that the RKB stopped movement. With the vertical movement of cylinder, RKB seeds flowed out of the cylinder and produced displacements in lateral and vertical directions to make a cone (Figure 9d).

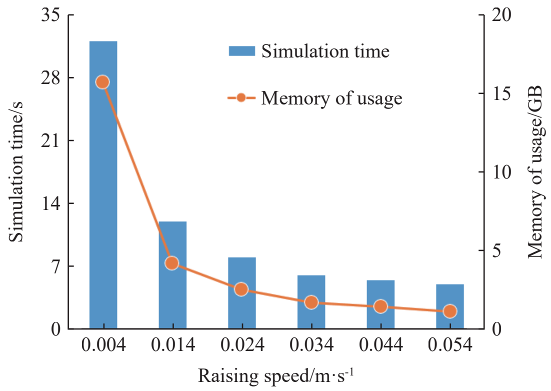

Figure 8 Effect of lifting velocity on simulation time and memory of usage

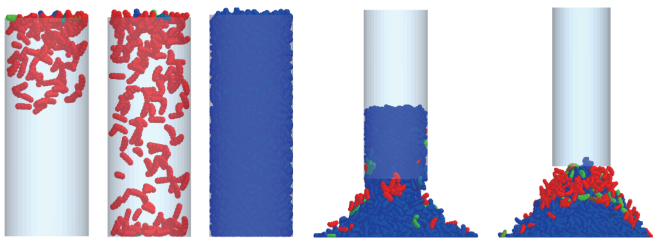

a. 0.13 s b. 0.23 s c. 1.9 s d. 7 s e. 8.5 s

Note: The red, green, and blue colors stand for the RKB seeds with high, low, and zero velocities, respectively.

Figure 9 Cone formation process of red kidney bean (RKB) at different moments

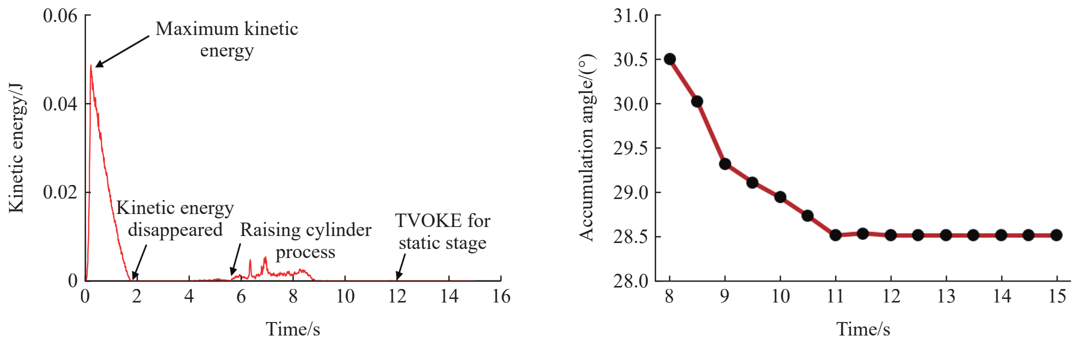

a. b.

Note: TVOKE represents threshold value of kinetic energy.

Figure 10 Variations of kinetic energies of red kidney bean (a) and accumulation angles with time (b)

RKB seeds kept moving when all of them flowed out of the cylinder, as indicated by RKB seeds with high velocities (Figure 9e) and some kinetic energies of RKB seeds (Figure 10a). By contrast, the RPA initially decreased gradually and then reached a static stage (Figure 10b). Threshold value of kinetic energy (TVOKE) for determining the static stage of RKB cone is quite important as it affects measurement accuracy of RPA and cost of simulation time and memory of usage. Too large or too small values of TVOKE can result in inaccurate RPA and rapid increase in simulation time (Figure 10b) and memory of usage, respectively. A TVOKE of 1×10^{-6} J is small enough in accordance with the study from Qi et al.[24] and was used for determining the static stage of RKB cone. It was found that kinetic energy was smaller than 1×10^{-6} J all the time after the moment of 12 s, and RPA was also quite stable. The moment of 12 s was therefore determined for RPA measurement.

3.3 Calibration of DEM parameters of RKB

3.3.1 Determination of significant DEM parameters

RPAs at various combinations of DEM parameters from

Plackett-Burman (PLB) test are listed in Table 3. The significance analysis showed that RPA was significantly affected by parameters *C* (coefficient of static friction between RKB seeds) and *D* (coefficient of rolling friction between RKB seeds) (p<0.05) (Table 4). The significance for effects of these parameters on RPA followed the rank in accordance with the Pareto Chart in Figure 11: $C > D > A > B > E > H > G > F$. Moreover, all of these parameters have positive effects on the RPA. To further obtain more reasonable ranges of significant parameters (i.e., *C* and *D*), steepest ascent (STA) test was carried out and listed in Table 5. With the increase in parameters *C* and *D*, RPA from DEM simulations was raised and the second combination resulted in the smallest relative error (3.1%) as compared with measured RPA of 22.1°. Therefore, more reasonable value ranges of *C* and *D* were 0.1-0.16 and 0.02-0.04 respectively, which were used in the following Central Composite (CEC) test to provide a basis for optimizing significant DEM parameters.

Table 3 Design scheme and results of Plackett-Burman test

No.	*A*	*B*	*C*	*D*	*E*	*F*	*G*	*H*	Repose angle/(°)
1	0.2	17	0.7	0.02	0.37	0.59	0.16	0.19	33.2
2	0.4	17	0.7	0.02	0.13	0.22	0.16	0.19	31.4
3	0.2	17	0.1	0.22	0.37	0.22	0.16	0.55	22
4	0.4	13	0.7	0.22	0.37	0.22	0.02	0.19	44.5
5	0.4	13	0.1	0.02	0.37	0.22	0.16	0.55	19.3
6	0.4	17	0.1	0.22	0.37	0.59	0.02	0.19	24.5
7	0.4	13	0.7	0.22	0.13	0.59	0.16	0.55	48.3
8	0.4	17	0.1	0.02	0.13	0.59	0.02	0.55	18.8
9	0.4	13	0.1	0.22	0.13	0.59	0.16	0.19	22
10	0.2	13	0.1	0.02	0.13	0.22	0.02	0.19	19.3
11	0.2	17	0.7	0.22	0.13	0.22	0.02	0.55	42.73
12	0.2	13	0.7	0.02	0.37	0.59	0.02	0.55	30.7
13	0.3	15	0.4	0.12	0.25	0.4	0.09	0.37	32.6

Table 4 Significance analysis of tested parameters

Parameter	Mean square	*df*	Sum of squares	*F*-value	*p*-value
Model	148.73	8	523.32	9.06	0.0484*
A	24.28	1	24.28	1.48	0.3110
B	11.35	1	11.35	0.6910	0.4668
C	921.03	1	921.03	56.07	0.0049**
D	221.28	1	221.28	13.47	0.0350*
E	6.06	1	6.06	0.3692	0.5864
F	0.1951	1	0.1951	0.0119	0.9201
G	1.42	1	1.42	0.0865	0.7878
H	4.24	1	4.24	0.2579	0.6465

Note: ** means extremely significant effect; * means significant effect (p<0.05).

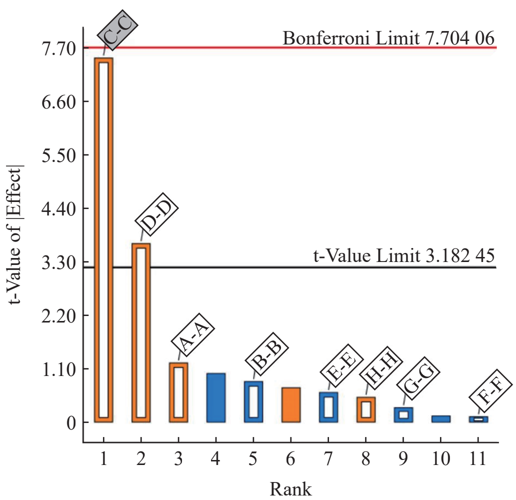

Figure 11 Pareto chart

Table 5 Design and results of steepest ascent test

No.	*C*	*D*	Repose angle/(°)	Relative error/%
1	0.1	0.02	20.9	8.3
2	**0.13**	**0.03**	**22.1**	**3.1**
3	0.16	0.04	24.1	5.7
4	0.22	0.06	28.5	25
5	0.34	0.10	32.9	44.29
6	0.46	0.14	39.1	71.49
7	0. 58	0.18	42.9	88.15
8	0.7	0.22	43.8	92.11

3.3.2 Optimization of DEM parameters

RPA values from CEC test are listed in Table 6. The relationship between RPA and significant parameters (i.e., *C* and *D*) was fitted based on these data as follows:

$$RPA = 21.88 + 1.36C + 0.5015D - 0.1125CD + 0.1396C^2 + 0.5569D^2 \tag{4}$$

Table 6 Central composite design and results

No.	*C*	*D*	RPA/(°)
1	−1 (0.1)	−1 (0.02)	20.9
2	1 (0.16)	−1	23.5
3	−1	1 (0.04)	21.95
4	1	1	24.1
5	−1.414 (0.088)	0 (0.03)	19.95
6	1.414 (0.172)	0	24.3
7	0 (0.13)	−1.414 (0.016)	22.12
8	0	1.414 (0.044)	23.79
9	0	0	22.1
10	0	0	21.6
11	0	0	21.58
12	0	0	21.89
13	0	0	22.24

Firstly, an objective function is defined as the absolute value of the relative error between the predicted RPA from Equation (4) and the measured RPA. The design variables are the two significant DEM parameters (*C* and *D*). The goal is to find the optimal parameter combination that minimizes this objective function. The second step is initialization of two algorithms, i.e., GWO and FPA. Each algorithm starts by generating an initial population of candidate solutions. Each candidate is a vector representing a specific set of the two DEM parameters. The third step is iterative search and evaluation. For each candidate solution, the objective function is calculated. This involves inputting the candidate parameter set into the pre-trained response surface model to instantly obtain a predicted RPA, then computing its absolute relative error against the measured value. This is computationally efficient because it replaces the requirement for a full EDEM simulation at this stage. Guided by their unique bio-inspired mechanisms, the algorithms update the positions of candidate solutions (i.e., adjust parameter sets) to explore search space more effectively. The fourth step is convergence. The run for each optimization process stops upon reaching the predefined 1000 iterations. This is sufficiently high to allow convergence.

The optimal combinations of significant DEM parameters obtained from the two algorithms are presented in Table 7. The relative error (RE) between predicted and simulated RPAs decreased with the increase in number of iterations for the two different swarm intelligence optimization algorithms (SIOAs) (Figure 12). REs at the initial iterations were 0.02% and 0.03% for GWO and FPA, respectively. Number of iterations with RE of

<0.0001% was smaller for the FPA; i.e. 36 iterations. Moreover, REs after 1000 iterations from GWO and FPA were comparatively small, indicating the FPA outperformed the GWO by comprehensively considering both efficiency and accuracy.

The cone images of RKB simulated by discrete element models obtained through the two different optimization algorithms are shown in Figures 13b and 13c. The RPAs were 22.4° and 21.9° for GWO and FPA, respectively. As compared with the actually measured RPA (22.1°), the relative error (RE) of simulated RPA optimized using FPA was 0.90%, which was smaller than that from GWO (1.36%), providing better accuracy of simulated RPA. To further verify the optimization results, the simulated RPA using DEM parameters optimized by FPA and measured RPA was analyzed using T-test. A p-value of >0.05 was obtained, indicating that the difference between actually measured RPA of 22.1° in Figure 13a and simulated RPA (21.9°) using DEM parameters optimized by FPA did not reach a significant level. The DEM parameters of RKB optimized by FPA were therefore effective and accurate. The validation method has been successively used in studies of Wang et al.[5] and Liu et al.[25]

Table 7 Optimization results from two different swarm intelligence optimization algorithms (SIOA)

SIOA	Optimal combination		Number of iterations with relative error (RE) of <0.0001%	RE after 1000 iterations/%
	C	D		
Grey wolf optimizer	0.1333	0.0200	840	0.85×10^{-6}
Flower pollination algorithm	0.1338	0.0308	36	1.04×10^{-6}

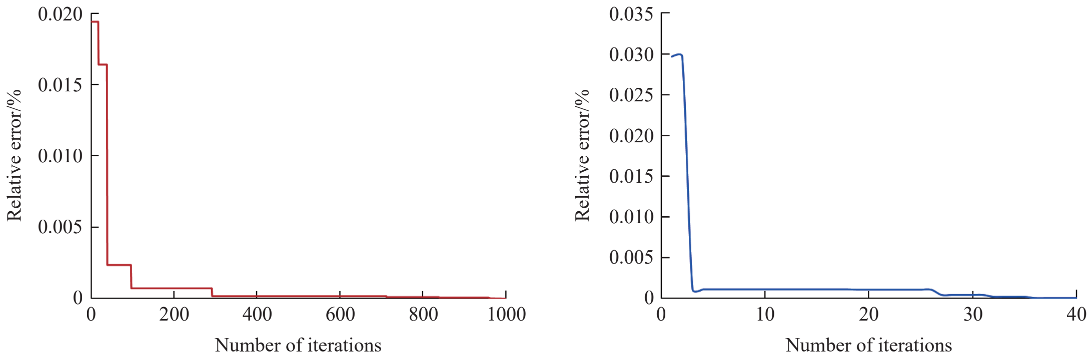

a. Grey wolf optimizer b. Flower pollination algorithm

Figure 12 Variation of relative error at various numbers of iterations

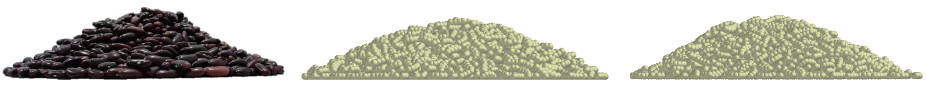

a. Actual measurement b. Simulations with DEM and GWO c. Simulations with DEM and FPA

Figure 13 RKB cone images from actual measurement and simulations with DEM parameters optimized using GWO and FPA

3.4 Discussion and implications

Before this study, most DEM parameters for RKBs—specifically eight key parameters—had not been reported. Calibrating these parameters using the conventional trial-and-error method (TEM) is typically inaccurate or inefficient[5].

Liu et al.[26,27] calibrated DEM parameters of alfalfa seeds and granular organic fertilizer, respectively, using a combination of Plackett-Burman (PB) design, Steepest Ascent test, Quadratic Orthogonal Rotatable Composite (QORC) or Box-Behnken design, and the Response Surface Method (RSM). Their reported relative errors ranged from 2.89% to 4.28%, which are considerably higher than the relative error of this study (0.9%). Zhang et al.[16] calibrated DEM parameters of mung bean seeds using a combination of the Steepest Ascent test, QORC design, and RSM. While their calibration efficiency was comparable, the absence of parameter screening via the PB test resulted in a higher relative error of 4.94%. Wu et al.[15] calibrated DEM parameters of peanut seeds using a full-factorial design. Only two random DEM parameters (i.e., CSF between peanut seeds and CRF between peanut seeds) were calibrated. The significant DEM parameters were not screened, resulting in a much larger relative error of 8.24%. In other words, to reduce the final relative error between simulated and measured RPAs, a total of 6561 simulations (i.e., 3^8) are required for a single full factorial test to calibrate eight DEM parameters of agricultural particles. The corresponding calibration efficiency is much lower. Similarly, Chen et al.[28] calibrated eight DEM parameters of pod pepper seeds using a Box-Behnken design test. A total of 120 combinations of DEM parameters were obtained for an eight-factor and three-level test design, indicating 360 simulations are required for the calibration (three repetitions for a set of DEM parameters). Although the difference between simulated and measured RPAs did not reach a significant level (p>0.05), the relative error between simulated and measured RPAs is 2.98%, which is more than twice that of this study. Moreover, the much larger number of simulations required greatly affects the calibration efficiency.

Most previous studies employing the method of combination of tests (MCT) did not validate their results using significance analysis to confirm the difference between simulated and measured RPAs. More importantly, the calibration accuracies achieved in those studies were generally lower than those obtained here. In contrast, the application of SIOAs in our study provided a superior search strategy compared to standard RSM optimizers from the literature. This increased the confidence that identified parameters are the best possible within the domain described by the Central Composite model, leading to a more accurate calibration foundation. We deliberately formulated the objective function as the absolute relative error. This is a more direct and intuitive measure of calibration accuracy than simply matching a target value, as it penalizes deviations proportionally and is the standard metric for evaluating prediction performance. Additionally, employing two different SIOAs allows for a comparative performance analysis of different search strategies for the DEM calibration issue. It mitigates the risk of relying on a single algorithm's performance and provides insights into which biological metaphor might be most effective for this class of inverse problems. Thus, the optimization method proposed in this study improved model accuracy.

Overall, the proposed calibration framework provides a reliable and efficient reference for accurately determining DEM parameters of various crop seeds and can contribute to the development and optimization of RKB-related agricultural machinery.

4 Conclusions

DEM parameters of red kidney beans (RKBs) are essential for understanding interactions between RKBs and agricultural machineries. In the study, the repose angle affected by lifting velocity and measuring moment in raising cylinder method (RCM) simulations was investigated. DEM parameters of RKBs were calibrated by a combination of Plackett-Burman, Steepest Ascent, and Central Composite tests and two typical swarm intelligence optimization algorithms. The following conclusions were drawn:

(1) Accurate repose angles of RKBs can be obtained efficiently when the threshold of kinetic energy is reached. Computation time, memory of usage, and lateral movement of RKB particles during RCM simulations were affected by lifting velocity and moment for repose angle (RPA) measurement. Moment of 12 s for RPA measurement and lifting velocity of 0.014 m/s were determined on aspects of higher accuracy in measuring repose angles and relatively less computation time and memory of usage in RCM simulations.

(2) An optimal combination of DEM parameters of RKBs is coefficient of static friction of 0.1338 and coefficient of rolling friction of 0.0308 optimized using the FPA.

(3) FPA outperformed the grey wolf optimizer by comprehensively considering both efficiency and accuracy. Relative error between actually measured RPA of 22.1° and simulated RPA (21.9°) using DEM parameters optimized by FPA was only 0.90%; the difference between these two RPAs did not reach a significant level, indicating that optimized DEM parameters have a good accuracy.

(4) The present study may be extended to other agricultural granular materials and provide a basis for investigating interactions between RKBs and related agricultural machineries. Future work will consider investigating the movement characteristics of the red kidney bean population and the interaction between it and the seed-metering device under different conditions (e.g., different forward speeds, vibration conditions, etc.) and optimizing the structural parameters of the seed-metering device.

Acknowledgements

This research was financially supported by National Natural Science Foundation of China (Grant No. 32401718), Outstanding Youth Science and Technology Cultivation Fund of Henan University of Science and Technology (Grant No. 2025HNKJ DXYXQNCXRC30), and Heluo Young Talent Supporting Project (Grant No. 2026HLTJ42).

[References]

[1] Zheng B F, Jiang L W, Li X Y, Liao L Y, Tian P K, Li S R. White spot and degree of damage control technology research in the manufacturing process of kidney bean cans. Hunan Agric. Sci., 2021; 7: 70–74. (in Chinese)

[2] Li T. Experimental study on biomechanical properties of miscellaneous bean seeds and design of air-suction seed metering device. Master thesis, Shanxi Agricultural University, China, 2022. (in Chinese)

[3] Ma D X, Shi S, Li H, Wei G J, Zhou J L, Shi Y P, et al. DEM-CFD-based simulation and optimization of a combined pneumatic-centrifugal wheat seed-metering device. Int J Agric & Biol Eng, 2025; 18(5): 127–141.

[4] Liu C J, Zhao W Y, Feng B, Shi L R, Sun B G, Dai F, et al. Calibration of DEM parameters for coated sunflower seeds based on dynamic stacking angle. Int J Agric & Biol Eng, 2026; 19(1): 283–294.

[5] Wang X Z, Zhang Q K, Huang Y X, Ji J T. An efficient method for determining DEM parameters of a loose cohesive soil modelled using hysteretic spring and linear cohesion contact models. Biosyst. Eng., 2022; 215: 283–294.

[6] Zeng Z W, Ma X, Cao X L, Li Z H, Wang X C. Critical review of applications of discrete element method in agricultural engineering. Transactions of the CSAM, 2021; 52(4): 1–20. (in Chinese)

[7] Wang X Z, Gu K Y, Dai F, Lokker C, Zeng Z W. Efficient calibration of discrete element method parameters for garbanzo beans using swarm intelligence optimization algorithms. Inf. Process. Agric, 2026, In Press. DOI: 10.1016/j.inpa.2026.01.014.

[8] Shi F G, Wu M L, Zhao Z H, Chen H Y, Jiang X H, Quan W. Calibration of rototilled soil block discrete element parameters after rotary tillage in rape planting by machinery. Int J Agric & Biol Eng, 2026; 19(2): 28–38.

[9] Yang Y W, Li M, Tong J, Ma Y H. Study on the interaction between soil and the five-claw combination of a mole using the discrete element method. Appl. Bionics Biomecha, 2018; 2018: 7854052.

[10] Ucgul M, Fielke J M, Saunders C. Defining the effect of sweep tillage tool cutting edge geometry on tillage forces using 3D discrete element modelling. Inf. Process. Agric., 2015; 2(2): 130–141.

[11] Yang H, Guo D L, Zhai Y B, Liang J H. Performance analysis and parameter optimization of peanut digging shovel operation based on discrete element analysis. Inf. Process. Agric., 2026; 13(1): 86–99.

[12] Zhu J Z, Zou M, Liu Y S, Gao K, Su B, Qi Y C. Measurement and calibration of DEM parameters of lunar soil simulant. Acta Astronautica, 2022; 191: 169–177.

[13] Li Y X, Li F X, Xu X M, Shen C P, Meng K P, Chen J, et al. Parameter calibration of wheat flour for discrete element method simulation based on particle scaling. Transactions of the CSAE, 2019; 35(16): 320–327. (in Chinese)

[14] Hu M J, Xia J F, Zhou Y, Luo C M, Zhou M K, Liu Z Y. Measurement and calibration of the discrete element parameters of coated delinted cotton seeds. Agriculture, 2022; 12(2): 286.

[15] Wu M C, Cong J L, Yan Q, Zhu T, Peng X Y, Wang Y S. Calibration and experiments for discrete element simulation parameters of peanut seed particles. Transactions of the CSAE, 2020; 36(23): 30–38. (in Chinese)

[16] Zhang S W, Zhang R Y, Chen T Y, Fu J, Yuan H F. Calibration of simulation parameters of Mung bean seeds using discrete element method and verification of seed-metering test. Transactions of the CSAM, 2022; 53(3): 71–79. (in Chinese)

[17] Sasmal B, Das A, Dhal K G, Saha R, Rai R, Bharasa T, Houssein E H. Artificial hummingbird algorithms: Theory, variants, analysis, applications, and performance evaluation. Computer Science Review, 2025; 56: 100727.

[18] Mirjalili S M, Lewis A. Grey wolf optimizer. Advances in Engineering Software, 2014; 69: 46–61.

[19] Yang X S, Karamanoglu M, He X S. Flower pollination algorithm: A novel approach for multiobjective optimization. Eng. Optimization, 2014; 46(9): 1222–1237.

[20] Zhang X J, Wang H T, Wang F Y, Lian Z G. Parameter calibration of discrete element model for alfalfa seeds based on EDEM simulation experiments. Int J Agric & Biol Eng, 2024; 17(3): 33–38.

[21] Chen Z P, Wassgren C, Veikle E, Ambrose K. Determination of material and interaction properties of maize and wheat kernels for DEM simulation. Biosyst. Eng., 2020; 195(C): 208–226.

[22] EDEM User Guide. DEM Solutions Ltd. Edinburgh, UK, 2014.

[23] Zhao H B, Huang Y X, Liu Z D, Liu W Z, Zheng Z Q. Applications of discrete element method in the research of agricultural machinery: A review. Agriculture, 2021; 11(5): 425.

[24] Qi L, Chen Y, Sadek M. Simulations of soil flow properties using the discrete element method (DEM). Comput. Electron. Agric., 2019; 157: 254–260.

[25] Liu F Y, Zhang J, Li B, Chen J. Calibration of parameters of wheat required in discrete element method simulation based on repose angle of particle heap. Transactions of the CSAE, 2016; 32(12): 247–253. (in Chinese)

[26] Liu H Y, Lu Q, Wang J W, Zhou W Q, Wang N H. Rapid calibration method for discrete element simulation parameters of columnar granular organic fertilizer with variable moisture content. Powder Technol, 2024; 448: 120354.

[27] Ma W P, You Y, Wang D C, Yin S J, Huan X L. Parameter calibration of alfalfa seed discrete element model based on RSM and NSGA-Ⅱ. Transactions of the CSAM, 2020; 51(8): 136–144. (in Chinese)

[28] Chen X Y, Wang X Z, Bai J, Fang W Q, Hong T Y, Zang N, et al. Virtual parameter calibration of pod pepper seeds based on discrete element simulation. Heliyon, 2024; 10(11): e31686.